Stem Cell Research & Therapy

RESEARCH

Open Access

Enhancing myelinogenesis through LIN28A rescues impaired cognition in PWMI mice

Xuan Wu[1], Zhechun Hu[2,9,10], Huimin Yue[3], Chao Wang[4], Jie Li[1], Yinxiang Yang[5], Zuo Luan[5], Liang Wang[6,9,10], Ying Shen[7,8] and Yan Gu[1,9,10*]

Abstract

Background In premature newborn infants, preterm white matter injury (PWMI) causes motor and cognitive disabilities. Accumulating evidence suggests that PWMI may result from defected differentiation of oligodendrocyte precursor cells (OPCs) and impaired maturation of oligodendrocytes. However, the underlying mechanisms remain unclear.

Methods Using RNAscope, we analyzed the expression level of RNA-binding protein LIN28A in individual OPCs. Knockout of one or both alleles of *Lin28a* in OPCs was achieved by administrating tamoxifen to $NG2^{CreER}$::Ai14::$Lin28a^{flox/+}$ or $NG2^{CreER}$::Ai14::$Lin28a^{flox/flox}$ mice. Lentivirus expressing FLEX-*Lin28a* was used in $NG2^{CreER}$ mice to overexpress LIN28A in OPCs. A series of behavioral tests were performed to assess the cognitive functions of mice. Two-tailed unpaired t-tests was carried out for statistical analysis between groups.

Results We found that the expression of *Lin28a* was decreased in OPCs in a PWMI mouse model. Knockout of one or both alleles of *Lin28a* in OPCs postnatally resulted in reduced OPC differentiation, decreased myelinogenesis and impaired cognitive functions. Supplementing LIN28A in OPCs postnatally was able to promote OPC differentiation and enhance myelinogenesis, thus rescuing the cognitive functions in PWMI mice.

Conclusion Our study reveals that LIN28A is critical in regulating postnatal myelinogenesis. Overexpression of LIN28A in OPCs rescues cognitive deficits in PWMI mice by promoting myelinogenesis, thus providing a potential strategy for the treatment of PWMI.

Keywords Preterm white matter injury, LIN28A, Oligodendrocyte, Oligodendrocyte precursor cells

*Correspondence:
Yan Gu
guyan2015@zju.edu.cn
[1] Center of Stem Cell and Regenerative Medicine, and Department of Neurology of the Second Affiliated Hospital, Zhejiang University School of Medicine, Hangzhou 310058, China
[2] School of Brain Science and Brain Medicine, Zhejiang University, Hangzhou 310058, China
[3] Department of Neurology of the First Affiliated Hospital, Interdisciplinary Institute of Neuroscience and Technology, Zhejiang University School of Medicine, Hangzhou 310027, China
[4] Department of Neurology of the Second Affiliated Hospital, Zhejiang University School of Medicine, Hangzhou 310058, China
[5] Department of Pediatrics, the Sixth Medical Center of PLA General Hospital, Beijing 10048, China
[6] Department of Neurology of the Second Affiliated Hospital and Department of Human Anatomy, Histology and Embryology, System Medicine Research Center, Zhejiang University School of Medicine, Hangzhou 310058, China
[7] International Institutes of Medicine, Department of Neurology, the Fourth Affiliated Hospital, Zhejiang University School of Medicine, Yiwu 322000, China
[8] Department of Physiology and Department of Psychiatry, Sir Run Run Shaw Hospital, Zhejiang University School of Medicine, Hangzhou 310058, China
[9] MOE Frontier Science Center for Brain Science & Brain-Machine Integration, Zhejiang University, Hangzhou 310058, China
[10] NHC and CAMS Key Laboratory of Medical Neurobiology, Zhejiang University School of Medicine, Hangzhou 310058, China

Background

Preterm white matter injury (PWMI) is a prevalent form of brain injury in premature newborns, particularly those with low birth weight [1], and has been a leading cause of motor and cognitive impairments in preterm children for decades [2–4]. Although the mechanisms of PWMI remain incompletely understood, a growing body of evidence suggests that PWMI may arise from aberrant differentiation of oligodendrocyte precursor cells (OPCs) and abnormal maturation of oligodendrocytes (OLs) [5]. Thus, transplanting optimized OPCs or optimizing endogenous OPCs to promote myelination in the brain has been considered as potential therapeutic strategies for treating PWMI [6].

LIN28 is an RNA-binding protein that controls self-renewal and differentiation of stem cells, as well as various biological processes [7]. Both LIN28 homologs A and B (LIN28A and LIN28B) block the biogenesis of miRNA *let-7* isoforms, and jointly determine cell lineage differentiation by counteracting each other [8]. In the mammalian nervous system, LIN28 plays important roles in regulating neural stem cell proliferation and differentiation during early brain development [9]. Our previous study has demonstrated that increased expression of LIN28A promotes neural stem cell differentiation towards neuronal fate and facilitates neuronal development [10]. On the other hand, it has been reported that *let-7* is able to regulate neurogliogenesis [11, 12]. In the peripheral nervous system, sustained expression of LIN28B in Schwann cells blocks *let-7* biogenesis and results in failure of myelination. Whereas, *let-7* accumulation promotes expression of the myelination-driving master transcription factor Krox20 by suppressing Notch signaling, thus supporting myelin formation [13]. However, it remains unclear whether LIN28 regulates the differentiation of OPCs, as well as the maturation and myelination of OLs in the context of the central nervous system.

Here we demonstrate that LIN28A plays a critical role in the regulation of OPC differentiation and OL myelination in the brain. The expression of LIN28A is reduced in OPCs in a mouse model of PWMI. Supplementing LIN28A in OPCs promotes myelination and at least partially rescues cognitive deficits in PWMI mice. Therefore, our study provides a potential strategy for the treatment of PWMI.

Methods

Animals

All procedures were approved by the Animal Care and Use Committee at Zhejiang University School of Medicine and were conducted in accordance with the policies of institutional guidelines on the care and use of laboratory animals. Mice were maintained at a 12 h light/dark cycle and group-housed in the animal facility of Zhejiang University School of Medicine, with free access to normal food and water. Both male and female mice were equally used.

Lin28a$^{flox/flox}$ mice (stock no. 023913), Ai14 reporter line (stock no. 007914) and NG2^{CreERT2} (stock no. 008538) were from Jackson Labs. These transgenic mouse lines were all maintained in C57BL/6 genetic background.

Aim, design and setting of the study

The aim of the study was to search for a strategy to optimize OPCs in vivo to rescue cognitive deficits in a PWMI mouse model.

We first assessed the cognitive impairments in a PWMI mouse model. Then we identified the changes in the expression level of *Lin28a* and *Lin28b* in OPCs after PWMI. To investigate the regulatory roles for LIN28A in myelinogenesis, we specifically deleted *Lin28a* gene from OPCs, then assessed the oligodendrogenesis and cognitive functions in these animals. Lastly, we tested whether overexpressing *Lin28a* in OPCs in vivo could rescue myelinogenesis and cognitive functions in PWMI mice.

A PWMI mouse model

As described previously [14], mouse pups at postnatal day 3 (P3) were anesthetized with isoflurane and then fixed ventral side up with micropore surgical tape while keeping the nasal mask in position. A 0.2–0.3 cm incision was made in the neck close to the midline. The left common carotid artery was isolated and ligated with 7/0 surgical silk sutures. The wound was sutured and then pups were allowed to recover from anesthesia on a heating pad. Pups were then placed in a hypoxic chamber with an oxygen concentration of 8% for 1.5 h. Finally, the pups were returned to their homecages and maintained under normal condition. Sham animals received the same procedure but without ligation of the left common carotid artery and hypoxia. Analgesia was achieved by local application of Xylocain during the procedure, and continued for 3 days after surgery.

Tamoxifen administration

Tamoxifen (Tam, Sigma-Aldrich) was dissolved in vegetable oil containing 0.1% ethanol to a concentration of 50 mg/mL. For *Lin28a* knockout, Tam was administered by i.p. injection (50 mg/kg) every other day from P5 to P13. For *Lin28a* overexpression, Tam was administered daily from P15 to P17, after viral injection.

Virus production and injection

As previously described [10], *Lin28a* cDNA sequence was synthesized and subcloned in a reversed direction into a pHage-FLEX lentiviral plasmid vector to

make a Cre-dependent lentiviral plasmid vector pHage-FLEX-GFP-p2A-Lin28a. pHage-FLEX-GFP was used as control vector. Lentiviral backbone plasmid was co-transfected with helper plasmids to 293 T cells using Lipofectamine 2000 (Invitrogen). Culture medium was collected, then virus was purified and concentrated by ultracentrifugation.

Stereotactic viral injections were performed in accordance with the Guidelines by Zhejiang University Animal Care and Use Committee. In brief, mice were anesthetized with isoflurane and mounted on a stereotaxic frame. An incision was made to expose the skull, and a hole was drilled in the skull of the ipsilateral side which underwent PWMI. Lentivirus (200 nL) was then delivered into the corpus callosum (stereotaxic coordinates: 1.0 mm anterior, 0.6 mm lateral from bregma, and 1.65 mm ventral from skull surface). After viral injection, bone wax was applied to cover the hole, and the incision was sutured. Mice were then returned to their homecages after waking up, and then housed under standard conditions. Analgesia was achieved by local application of Xylocain during the procedure, and continued for 3 days after surgery. Viral injection site was verified post hoc after behavioral tests, and data from animals with wrong injection sites were excluded for analysis.

Behavioral tests

Open field test

Mice were placed in the center of a brightly illuminated open field (45 cm × 45 cm × 35 cm), and were allowed to freely explore for 10 min. The movement of the mice was recorded by an overhead camera. The distance traveled and time spent in the inner and outer zones were analyzed by ANYmaze 7.4 software.

Elevated plus-maze (EPM) test

Mice were placed in the center of an EPM with opposite open and closed arms, and were allowed to freely explore the maze for 10 min with their movements recorded by an overhead camera. The number of entrance and time spent in the open and closed arms were analyzed by ANYmaze 7.4 software.

Novel object recognition (NOR) test

As previously described [15], mice were placed in a normally illuminated box (45 cm × 45 cm × 35 cm) and allowed to habituate for 30 min before the training session. During the training session, two identical objects were place close to two corners in the box, and mice were allowed to freely explore for 10 min. An hour later, during the test session, mice were put back in the box, with one of the two identical objects replace with a different object (novel object). The exploration time of the mice on the novel and familiar objects was recorded by an overhead camera and analyzed offline by ANYmaze 7.4 software. The discrimination index was calculated as $time_{novel}/(time_{novel} + time_{familiar})$.

Novel location recognition (NLR) test

Mice were placed in a normally illuminated box (45 cm × 45 cm × 35 cm), and allowed to habituate for 30 min before the training session. During the training session, two identical objects were place close to two corners in the box, and mice were allowed to freely explore for 10 min. An hour later, during the test session, mice were put back in the box, with one of the two identical objects moved to a different location (novel location). The exploration time of the mice on the objects at novel and familiar locations was recorded by an overhead camera and analyzed offline by ANYmaze 7.4 software. The discrimination index was calculated as $time_{novel}/(time_{novel} + time_{familiar})$.

Morris water maze test

As described previously [16], Morris water maze test was conducted in a circular water maze tank (120 cm in diameter, 50 cm deep) containing opaque water (~ 25 ℃), with distinct cues painted on surrounding walls. A circular escape platform (10-cm diameter) was submerged 0.5 cm below the water surface at a fixed location in one quadrant. During the training period, mice were trained for 4 trials per day. In each trial, mice were placed into the pool from one of the four pseudorandom starting points. The trial was completed once the mice found the platform or 60 s had elapsed. During the test session, the mice were allowed to swim in the pool for 60 s, with the platform removed. The swimming traces of the mice during the training and test sessions were recorded and analyzed using an automated tracking system (Ethovision XT, Noldus).

Immunofluorescence staining and RNAscope

Immunofluorescence staining was conducted as previously described [10]. Mice were deeply anesthetized with phenobarbital, and perfused transcardially with 40 mL ice-cold phosphate buffer solution (PBS) followed by 25 mL of 4% paraformaldehyde (PFA). The brains were collected, fixed overnight in 4% PFA, and then transferred to a 30% sucrose solution. Coronal brain sections were made and then permeabilized with 0.2% Triton X-100, and blocked in 5% normal donkey serum. Regular immunostaining was performed using primary antibodies to oligodendrocyte transcription factor 2 (Olig2, Abcam, ab109186, 1:1000), platelet-derived growth factor receptor alpha (PDGFRα, R&D Systems, AF1062, 1:1000), myelin-associated glycoprotein (MAG, Santa Cruz,

sc-376145, 1:500), and Ki67 (Abcam, ab16667, 1:1000) overnight at 4 °C. Sections were then incubated with secondary antibodies donkey-anti-rabbit Cy2 (Jackson ImmunoResearch, 711-225-152, 1:1000), donkey-anti-mouse Cy3 (Jackson ImmunoResearch, 715–165-151, 1:1000), donkey-anti-goat Cy5 (Jackson ImmunoResearch, 705-175-147, 1:1000) for 2 h at room temperature (25 °C). After staining, sections were mounted on slides with Fluoromount-G anti-fade medium containing DAPI (SouthernBiotech).

For RNAscope, ethanol was used for gradient dehydration of the sections. In situ hybridization was then performed using RNAscope multiplex fluorescent reagent kit with RNA probes for *Lin28a* (Advanced Cell Diagnostics, 437,121) or *Lin28b* (Advanced Cell Diagnostics, 447,881), according to manufacturer's instructions. Additional immunostaining was done following standard protocols as described above.

Z-stack images were then taken on an Olympus FV3000 confocal microscope, and analyzed using ImageJ software.

Statistics analysis

Data were analyzed using GraphPad Prism 8.0 software. Kolmogorov–Smirnov Test was used to test the normality of data distribution. Unpaired two-tailed Student's parametric t-tests were then employed for analyzing statistical differences between groups with normal data distribution, or non-parametric t-tests were otherwise used for data not being normally distributed. Data were presented as Mean ± SD. Statistical significance was considered when $P < 0.05$.

Results

PWMI leads to cognitive impairments

We first established a mouse PWMI model using wildtype C57BL/6 mouse pups at P3, by unilateral carotid artery ligation followed by low oxygen exposure (8% O2) for 1.5 h as previously described [17, 18]. At P14, these pups exhibited reduced thickness of the corpus callosum and enlarged lateral ventricle in the ipsilateral side of the brain, which underwent carotid artery ligation (Fig. 1a). The ipsilateral-to-contralateral ratio was decreased in the thickness of corpus callosum, and increased in the area of lateral ventricles (Fig. 1b, c). These results indicate that the ipsilateral side of the brain experienced white matter injury.

We assessed the behaviors of these animals when they were at approximately 2.5 months of age. We found that PWMI mice displaced similar number of entries to and time spent in the center zone in the open field test (Suppl. Fig. S1a, b), as well as comparable total travel

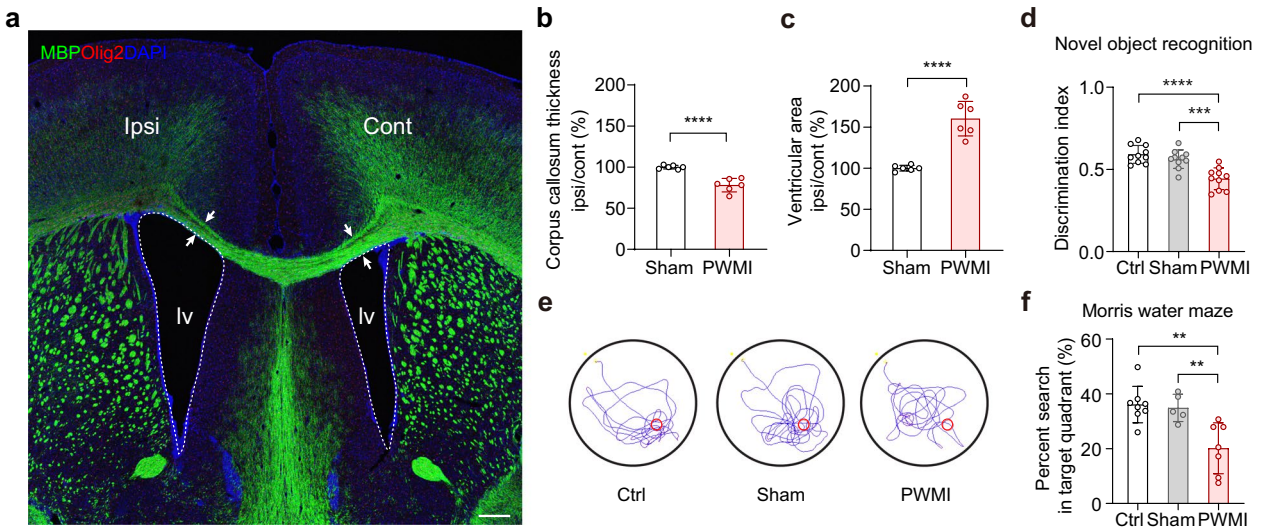

Fig. 1 PWMI leads to cognitive impairments. **a** Representative image showing thinner corpus callosum (indicated by arrows) and enlarged lateral ventricle (indicated by dashed lines) in the ipsilateral side of the brain after PWMI at P14. Ipsi: ipsilateral; Cont: contralateral; lv: lateral ventricle. Scale bar: 100 μm. **b** PWMI decreased the ratio of corpus callosum thickness (ipsi/cont) (Sham n = 6 mice, PWMI n = 6 mice; unpaired t test, $^{****}P < 0.0001$). **c** PWMI increased the ratio of lateral ventricle area (ipsi/cont) (Sham n = 6 mice, PWMI n = 6 mice; unpaired t test, $^{****}P < 0.0001$). **d** PWMI mice showed impaired discrimination in the NOR tests (Ctrl n = 10 mice, Sham n = 10 mice, PWMI n = 10 mice; unpaired t test, Ctrl vs. PWMI: $^{****}P < 0.0001$; Sham vs. PWMI: $^{***}P = 0.0004$; Ctrl vs. Sham: $P = 0.2534$). **e** Representative swimming traces of mice in the Morris water maze during the test session. The red circle indicates the location of the platform during training sessions. **f** PWMI mice showed significantly less time spent in the target quadrant during the test session. (Ctrl n = 8 mice, Sham n = 5 mice, PWMI n = 7 mice; unpaired t test, Ctrl vs. PWMI: $^{**}P = 0.0020$; Sham vs. PWMI: $^{**}P = 0.0095$; Ctrl vs. Sham: $P = 0.7359$). Data are shown as Mean ± SD

distance (Suppl. Fig. S1c), when compared with Ctrl and Sham animals. When tested in an EPM, PWMI mice also exhibited similar number of entries to and time spent in the open arms, compared with Ctrl and Sham animals (Suppl. Fig. S1d, e). These data suggest that PWMI mice exhibit normal locomotion and anxiety level.

During the NLR test, PWMI mice exhibited a preference for the object at a novel location, with a discrimination index comparable to that of Ctrl and Sham animals (Suppl. Fig. S1f), indicating their intact ability to recognize a novel location. However, during the NOR test, PWMI mice did not display a preference for a novel object, as evidenced by a significantly decreased discrimination index compared to Ctrl and Sham mice (Fig. 1d), suggesting their impaired ability to recognize a novel object. Furthermore, in the Morris water maze test, PWMI mice spent significantly less time searching in the target quadrant during the test session (Fig. 1e, f). These findings indicate that PWMI impairs specific types of cognitive functions.

PWMI increased proliferation but decreased differentiation of OPCs

To find out the impact of PWMI on the generation of OLs, we conducted immunostaining for PDGFRα, MAG and Olig2, which are markers for OPCs, OLs and oligodendroglial lineage cells, respectively, in the corpus callosum (Fig. 2a) and cortex (Fig. 2b) at different developmental stages following PWMI. We observed a significant increase in the density of $Olig2^+PDGFR\alpha^+$ cells in the ipsilateral side of the brain in the corpus callosum at P7 and P14, compared to that in the contralateral side. No significant change was observed in the corpus callosum at P28 or in the cortex from P7 to P28 (Fig. 2c). However, there was a notable elevation in the percentage of $Olig2^+PDGFR\alpha^+$ cells within all $Olig2^+$ cells ($Olig2^+PDGFR\alpha^+/Olig2^+$) both in the corpus callosum and cortex at P7, P14 and P28 (Fig. 2d). Due to challenges with identifying MAG^+ cell bodies at P7, we analyzed the ipsilateral-to-contralateral ratio of MAG signal intensity, and found it lower than 100%, both in the corpus callosum and cortex (Fig. 2e). At P14 and P28, there was a reduction in both the density of MAG^+Olig2^+ cells (Fig. 2f) as well as the percentage of MAG^+Olig2^+ cells within all $Olig2^+$ cells (Fig. 2g) in the ipsilateral side compared to the contralateral side. These data indicate that PWMI increases the number and proportion of OPCs while decreasing those of OLs in the corpus callosum and cortex.

We subsequently investigated the impact of PWMI on the proliferation of OPCs by co-staining PDGFRα with a proliferation marker Ki67. We found a significant increase in the proportion of $Ki67^+PDGFR\alpha^+$ cells among all $PDGFR\alpha^+$ cells in the ipsilateral side at P7 and P14, while no difference was observed at P28 (Fig. 2h, i), indicating that PWMI promotes OPC proliferation during the early post-injury period. In addition, we did not observe significant difference in the colocalization of cleaved caspase 3 (cCasp3) with MAG^+ cells between contralateral and ipsilateral corpus callosum at P14 (Suppl. Fig. S2), suggesting that the apoptosis of OLs was not altered at this time point in this PWMI mouse model.

These data suggest that PWMI increases the proliferation OPCs, but hinders the differentiation of OPCs towards OLs, thus resulting in impaired myelinogenesis in both corpus callosum and cortex.

PWMI leads to decreased expression of *Lin28a* in OPCs in the postnatal brain

Since LIN28A and LIN28B play a critical role in the regulation of cellular proliferation and differentiation [19], we performed RNAscope to examine the impact of PWMI on the expression of *Lin28a* and *Lin28b* in OPCs by quantifying the number of dots labeled by

(See figure on next page.)

Fig. 2 PWMI increased proliferation but decreased differentiation of OPCs. **a** Representative images of immunofluorescent staining of PDGFRα and MAG in the ipsilateral (Ipsi) and contralateral (Cont) corpus callosum after PWMI at P7, P14 and P28. Scale bar: 50 μm. **b** Representative images of immunofluorescent staining of PDGFRα and MAG in the ipsilateral (Ipsi) and contralateral (Cont) cortex after PWMI at P7, P14 and P28. Scale bar: 50 μm. **c** PWMI increased the density of $Olig2^+PDGFR\alpha^+$ cells in the ipsilateral corpus callosum at P7 and P14. (P7 n = 15 mice, P14 n = 10 mice, P28 n = 8 mice; unpaired t test, corpus callosum: P7 *P = 0.0348; P14 *P = 0.0319; P28 P = 0.4842; cortex: P7 *P* = 0.1054; P14 P = 0.0774; P28 P = 0.6779). **d** PWMI increased the proportion of $Olig2^+PDGFR\alpha^+$ cells in $Olig2^+$ cells in the ipsilateral brain. (P7 n = 10 mice, P14 n = 10 mice, P28 n = 8 mice; unpaired t test, corpus callosum: P7 ***P* = 0.0009; P14 **P* = 0.0179; P28 ***P* = 0.0003; cortex: P7 **P* = 0.0368; P14 ***P* = 0.0096; P28 **P* = 0.0249). **e** PWMI decreased the relative fluorescence intensity of MAG in both corpus callosum and cortex at P7 (n = 10 mice). **f** PWMI decreased the density of $Olig2^+MAG^+$ cells in the ipsilateral brain. (P14 n = 10 mice, P28 n = 8 mice; unpaired t test, corpus callosum: P14 **P* = 0.0312; P28 **P* = 0.0198; cortex: P14 ***P* = 0.0073; P28 ***P* = 0.0005). **g** PWMI decreased the proportion of $Olig2^+MAG^+$ cells in $Olig2^+$ cells in the ipsilateral brain. (P14 n = 10 mice, P28 n = 8 mice; corpus callosum: P14 unpaired t test, **P* = 0.0247; P28 unpaired t test, **P* = 0.0156; cortex: P14 unpaired t test, **P* = 0.0226; P28 unpaired t test, **P* = 0.0428). **h** Representative images of immunofluorescent staining of PDGFRα and Ki67 in the ipsilateral (Ipsi) and contralateral (Cont) corpus callosum after PWMI at P7, P14 and P28. Arrows indicate $Ki67^+PDGFR\alpha^+$ cells. Scale bar: 50 μm. **i** The proportion of $Ki67^+PDGFR\alpha^+$ cells among all $PDGFR\alpha^+$ cells in the ipsilateral (Ipsi) and contralateral (Cont) corpus callosum after PWMI at P7, P14 and P28. (P7 n = 8 mice, P14 n = 8 mice, P28 n = 8 mice; unpaired t test, P7 **P* = 0.0318; P14 ***P* = 0.0045; P28 *P* = 0.6885). Data are shown as Mean ± SD

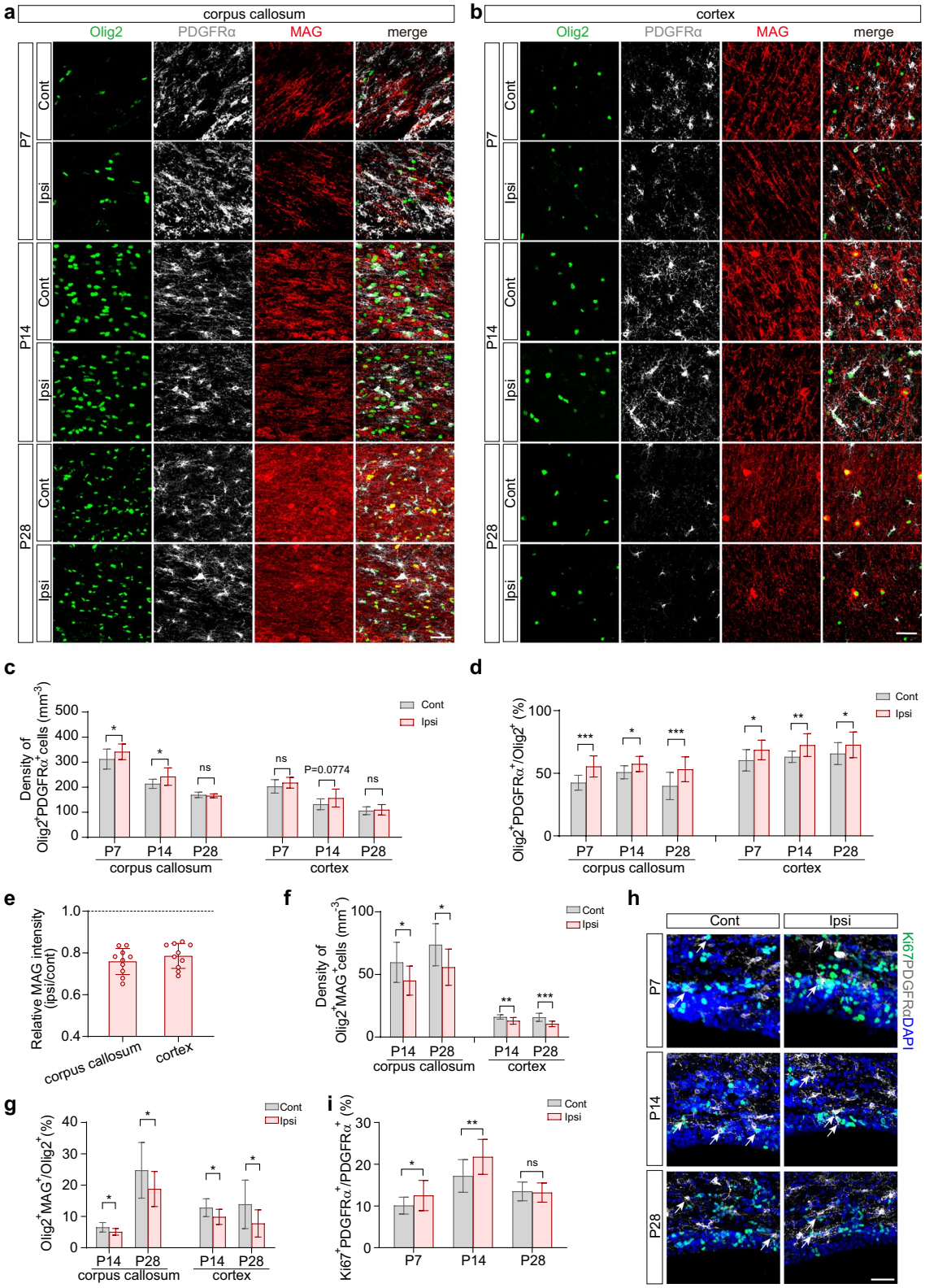

Fig. 2 (See legend on previous page.)

mRNA probes, as previously described [10]. We found that in Ctrl animals, the expression of *Lin28a* in OPCs reduced with postnatal development in normally developing mice (Fig. 3a, b), whereas PWMI led to a significant reduction of *Lin28a* expression in OPCs within the ipsilateral brain at each time point compared to Ctrl animals or the contralateral side of the brain (Fig. 3a, b). On the other hand, *Lin28b* expression remained consistently low in OPCs during postnatal brain development from P7 to P28, and did not show alterations following PWMI except for a decrease observed at P28 after PWMI (Fig. 3c, d). These data suggest that the reduced expression of *Lin28a* in OPCs may be associated with the impaired myelinogenesis in PWMI mice.

Loss of *Lin28a* in OPCs leads to decreased myelinogenesis and impaired cognitive functions

To find out the essential role of LIN28A in myelinogenesis, we administrated Tam every other day from P5 to P13 to NG2^{CreERT2}::Ai14::Lin28a$^{flox/flox}$ (flox/flox) and NG2^{CreERT2}::Ai14::Lin28a$^{flox/+}$ (flox/+) mice in order to delete both or one of the alleles of *Lin28a* in OPCs while labeling these cells and their progenies (Fig. 4a). NG2^{CreERT2}::Ai14 (+/+) littermates were used as controls. Using RNAscope, we found that *Lin28a* expression was significantly decreased in dTomato-labeled OPCs in flox/+ and flox/flox mice (Suppl Fig. S3). At P35, there was no significant change in the density of tdTomato^{+} cells in the corpus callosum or cortex of flox/flox mice, compared with +/+ or flox/+ mice (Fig. 4a, b). However,

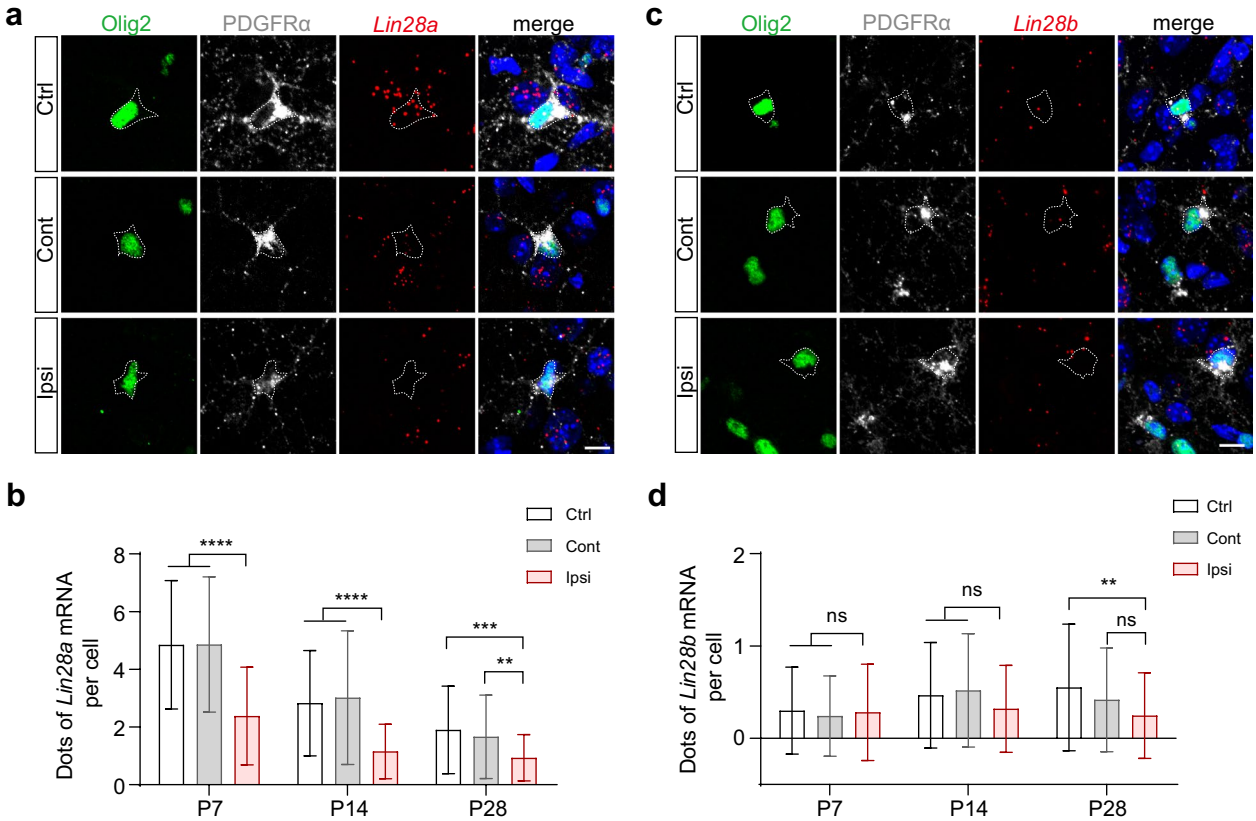

Fig. 3 PWMI leads to decreased expression of *Lin28a* in OPCs in the postnatal brain. **a** Representative RNAscope images showing *Lin28a* mRNA in PDGFRα^{+} cells in the cortex of Ctrl and PWMI mice at P14. Cell bodies are outlined by dotted lines. Scale bar: 10 μm. **b** *Lin28a* mRNA decreased in OPCs in the ipsilateral cortex of PWMI mice (P7: Ctrl n = 5 mice, Cont n = 5 mice, Ipsi n = 5 mice, unpaired *t* test, Ctrl vs. Ipsi ****$P < 0.0001$, Cont vs Ipsi ****$P < 0.0001$, Ctrl vs. Cont $P = 0.9801$; P14: Ctrl n = 8 mice, Cont n = 8 mice, Ipsi n = 8 mice, unpaired *t* test, Ctrl vs. Ipsi ****$P < 0.0001$, Cont vs Ipsi ****$P < 0.0001$, Ctrl vs. Cont P = 0.6602; P28: Ctrl n = 8 mice, Cont n = 8 mice, Ipsi n = 8 mice, unpaired *t* test, Ctrl vs. Ipsi ***$P = 0.0003$, Cont vs. Ipsi **$P = 0.0027$, Ctrl vs. Cont $P = 0.4267$). **c** Representative RNAscope images showing *Lin28b* mRNA in PDGFRα^{+} cells in the cortex of Ctrl and PWMI mice at P14. Cell bodies are outlined by dotted lines. Scale bar: 10 μm. **d** *Lin28b* mRNA did not significantly change in OPCs in the ipsilateral cortex of PWMI mice (P7: Ctrl n = 4 mice, Cont n = 4 mice, Ipsi n = 4 mice, unpaired *t* test, Ctrl vs. Ipsi $P = 0.8966$, Cont vs. Ipsi $P = 0.7487$, Ctrl vs. Cont $P = 0.6560$; P14: Ctrl n = 6 mice, Cont n = 6 mice, Ipsi n = 6 mice, unpaired *t* test, Ctrl vs. Ipsi $P = 0.2174$, Cont vs. Ipsi $P = 0.0707$, Ctrl vs. Cont $P = 0.7007$; P28: Ctrl n = 6 mice, Cont n = 6 mice, Ipsi n = 6 mice, unpaired *t* test, Ctrl vs. Ipsi **$P = 0.0099$, Cont vs. Ipsi $P = 0.0544$, Ctrl vs. Cont $P = 0.3257$). Data are shown as Mean ± SD

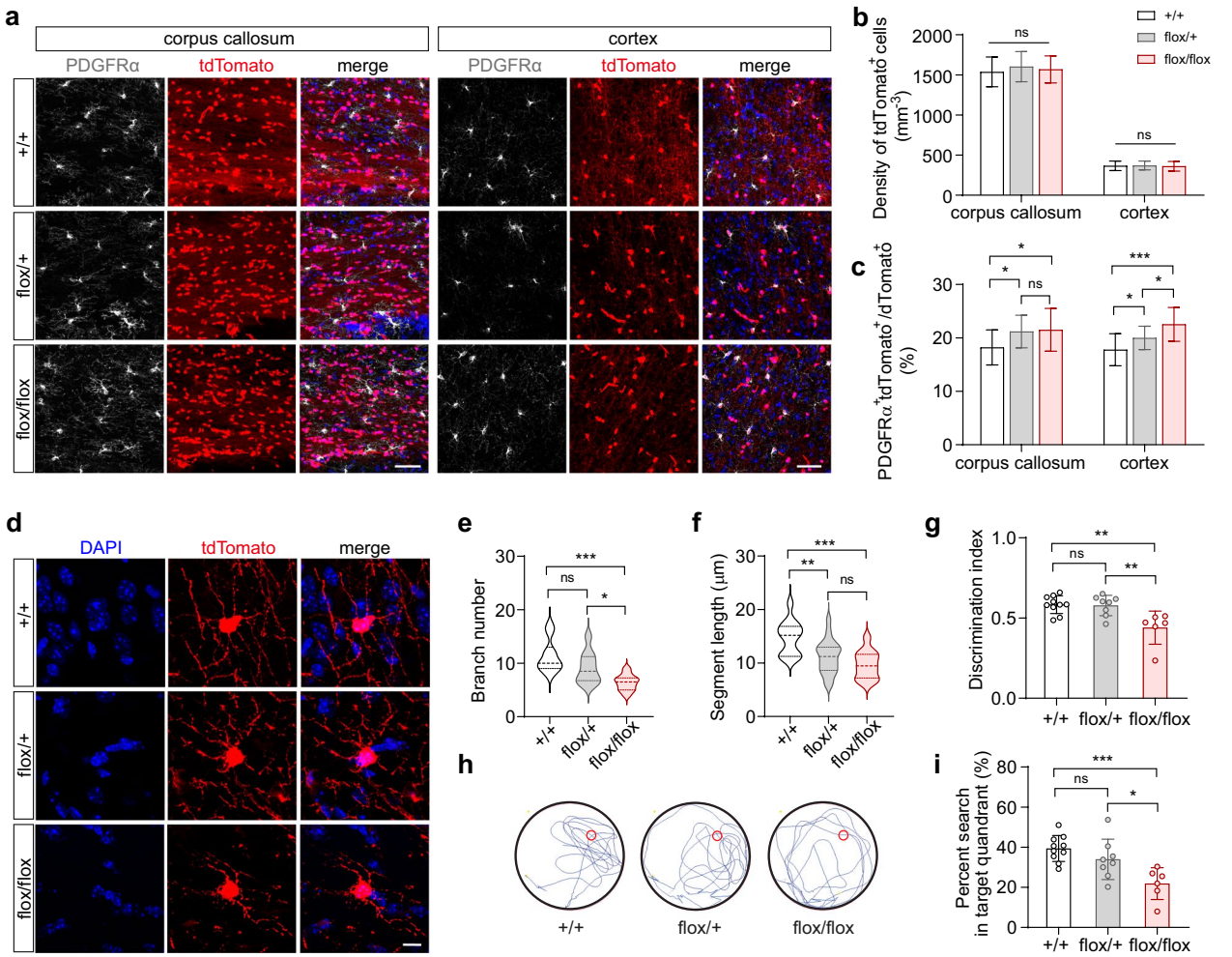

Fig. 4 Loss of LIN28A in OPCs leads to decreased myelinogenesis and impaired cognitive functions. **a.** Representative images of tdTomato$^+$ cells in the corpus callosum and cortex of NG2^{CreERT2}::Ai14 (+/+), NG2^{CreERT2}::Ai14::Lin28a$^{flox/+}$ (flox/+) and NG2^{CreERT2}::Ai14::Lin28a$^{flox/flox}$ (flox/flox) mice. Scale bar: 50 μm. **b** The density of tdTomato$^+$ cells in corpus callosum and cortex (+/+ n = 5 mice, flox/+ n = 5 mice, flox/flox n = 5 mice; unpaired t test, corpus callosum: +/+ vs. flox/flox $P = 0.6274$, flox/+ vs. flox/flox $P = 0.6058$, +/+ vs. flox/+ $P = 0.3428$; cortex: +/+ vs. flox/flox $P = 0.8028$, flox/+ vs. flox/flox $P = 0.6541$, +/+ vs. flox/+ $P = 0.8460$). **c** The proportion of PDGFRα$^+$tdTomato$^+$ among tdTomato$^+$ cells was increased in flox/+ and flox/flox mice (+/+ n = 5 mice, flox/+ n = 5 mice, flox/flox n = 5 mice; unpaired t test, corpus callosum: +/+ vs. flox/flox $^*P = 0.0199$, flox/+ vs. flox/flox $P = 0.8091$, +/+ vs. flox/+ $^*P = 0.0154$; cortex: +/+ vs. flox/flox $^{***}P = 0.0002$, flox/+ vs flox/flox $^*P = 0.0161$, +/+ vs. flox/+ $^*P = 0.0292$). **d** Representative images of tdTomato$^+$ cells in+/+, flox/+ and flox/flox mice. Scale bar: 10 μm. **e** Deleting *Lin28a* led to decreased number of branches from single OLs. (+/+ n = 30 cells from 5 mice, flox/+ n = 40 cells from 5 mice, flox/flox n = 30 cells from 5 mice; unpaired t test, +/+ vs. flox/flox $^{***}P = 0.0002$, flox/+ vs. flox/flox $^*P = 0.0182$, +/+ vs. flox/+ $P = 0.1152$). **f** Deleting *Lin28a* led to decreased segment length of myelin sheaths. (+/+ n = 193 segments from 5 mice, flox/+ n = 380 segments from 5 mice, flox/flox n = 178 segments from 5 mice; unpaired *t* test, +/+ vs. flox/flox $^{***}P = 0.0002$, flox/+ vs. flox/flox $P = 0.1755$, +/+ vs. flox/+ $^{**}P = 0.0034$). **g** Impaired NOR in flox/flox mice (+/+ n = 10 mice, flox/+ n = 8 mice, flox/flox n = 6 mice; unpaired *t* test, +/+ vs. flox/flox $^{**}P = 0.0026$, flox/+ vs. flox/flox $^{**}P = 0.0091$, +/+ vs. flox/+ $P = 0.8491$). **h** Representative swimming traces of +/+, flox/+ and flox/flox mice in the Morris water maze during the test session. The red circle indicates the location of the platform during training sessions. **i** flox/flox mice showed significantly less time spent in the target quadrant during the test session. (+/+ n = 10 mice, flox/+ n = 8 mice, flox/flox n = 6 mice; unpaired *t* test, +/+ vs. flox/flox $^{***}P = 0.0003$, flox/+ vs. flox/flox $^*P = 0.0317$, +/+ vs. flox/+ $P = 0.1849$). Data are shown as Mean ± SD

knockout of one or both alleles of *Lin28a* resulted in an increased proportion of PDFGRα$^+$tdTomato$^+$ cells within all tdTomato$^+$ cells in the corpus callosum and cortex (Fig. 4c). These data suggests that loss of LIN28A impedes the differentiation of OPCs towards OLs. Subsequently, we further analyzed the myelin sheaths formed by tdTomato$^+$ OLs in these animals at P35 (Fig. 4d). We found that tdTomato$^+$ OLs in flox/flox mice exhibited significantly fewer branches and shorter segment length of myelin sheaths compared to those in +/+ or flox/+ mice (Fig. 4e, f), indicating that loss of *Lin28a* in OPCs and OLs resulted in impaired myelination in the brain.

To find out whether loss of *Lin28a* in OPCs during postnatal development could alter cognitive functions, we tested the behaviors of these flox/flox mice, in parallel with their flox/+and+/+littermates, when they were around 2.5 months old. We found that flox/flox and flox/+mice exhibited similar number of entries to and time spent in the center zone in the open field (Suppl. Fig. S4a, b), as well as comparable total travel distance (Suppl. Fig. S3c), compared with+/+mice. In the EPM test, flox/flox and flox/+mice also exhibited similar number of entries to and time spent in the open arms, compared with+/+animals (Suppl. Fig. S4d, e). These data suggest that loss of one allele or both alleles of *Lin28a* in OPCs during postnatal development does not alter the locomotion or anxiety level in flox/+or flox/flox mice.

In the NLR test, flox/flox and flox/+mice showed preference for the object at a novel location with a discrimination index comparable to that of+/+animals (Suppl. Fig. S4f), indicating their normal ability to recognize a novel location. However, in the NOR test, flox/flox mice showed a significantly decreased discrimination index compared to+/+and flox/+mice (Fig. 4g), suggesting an impaired ability to recognize a novel object. Furthermore, in the Morris water maze test, flox/flox mice spent significantly less time searching in the target quadrant during the test session, compared to+/+and flox/+mice (Fig. 4h, i). These data suggest that loss of *Lin28a* in both alleles leads to cognitive impairments similar to those observed in PWMI mice.

Supplementing *Lin28a* in OPCs rescued myelinogenesis and cognitive functions in PWMI mice

We then wondered whether the defects in myelinogenesis and cognitive functions in PWMI mice could be recovered by over-expression of *Lin28a* in OPCs. Following PWMI in $NG2^{CreERT2}$ mice at P3, we infused lentivirus expressing FLEX-*Lin28a* (Lenti-CAG-FLEX-*Lin28a*-p2A-GFP) into the ipsilateral corpus callosum at P14. A lentivirus expressing GFP (Lenti-CAG-FLEX-GFP) was used as control. Tam was administrated daily from P15 to P17 to induce the expression of LIN28A or GFP only (Fig. 5a). Immunostaining showed that lentivirus (GFP^+) successfully labeled $PDGFR\alpha^+$ cells in the corpus callosum, and LIN28A expression was induced in virally-labeled cells in Lin28a group (Fig. 5b). No significant difference in the number of GFP^+Olig2^+ cells was found between the two groups (Fig. 5c, d), suggesting that similar number of oligodendroglial lineage cells were labeled in both groups using this strategy (Fig. 5a). However, among the GFP^+Olig2^+ cells, LIN28A overexpression significantly decreased the percentage of $PDGFR\alpha^+GFP^+Olig2^+$ cells within GFP^+Olig2^+ cells (Fig. 5c, e), but increased that of $PDGFR\alpha^-GFP^+Olig2^+$ cells (Fig. 5c, f). These data suggest that overexpression of LIN28A rescued the hindered OPC differentiation in the PWMI brain. Furthermore, GFP-labeled OLs in Lin28a group exhibited significantly increased branch number and segment length of myelin sheaths (Fig. 5g-i), suggesting that overexpression of LIN28A in OPCs recovered the defects in myelinogenesis observed in the PWMI brain.

Moreover, we found that the two group of mice showed comparable number of entries to and time spent in the center zone, as well as total travel distance during the open field test (Suppl. Fig. S5a-c). In the EPM test, both groups exhibited similar number of entries to and time spent in the open arms (Suppl. Fig. S5d, e). In the NLR test, the Lin28a group showed similar discrimination index compared to Ctrl animals (Suppl. Fig. S5f). Intriguingly, in the NOR test, mice in Lin28a group exhibited a stronger preference for a novel object, as evidenced by a significantly increased discrimination index compared to Ctrl mice (Fig. 5j), suggesting that their ability to recognize a novel object was recovered. In addition, in the Morris water maze test, the Lin28a group spent significantly longer time searching in the target quadrant during the test session, compared to Ctrl mice (Fig. 5k, l). These data suggest that overexpression of LIN28A in OPCs rescues the cognitive impairments observed in PWMI mice.

Discussion

PWMI is the most common form of injury among preterm infants [20]. Hypoxic-ischemic injury and inflammation are two primary risk factors contributing to PWMI [3, 21]. The peak incidence of PWMI occurs between 23 and 32 weeks of gestation, coinciding with a crucial period in the generation and development of OLs [22]. At this age, OPCs and premyelinating OLs (pre-OLs) are particularly susceptible to hypoxic and inflammatory insults [23]. Several animal models have been developed for the study of PWMI [24]. Unilateral common carotid artery ligation followed by hypoxia has been used to provide stable rodent PWMI models [14, 25]. In our study, using this PWMI mouse model, we found that the proliferation of OPCs was transiently elevated during the early stages post PWMI at P7 and P14, and returned to normal level by P28, which is consistent with previous studies on optic nerves [26]. Compared to the transiently elevated OPC proliferation, the defects in OPC differentiation and OL maturation lasted even longer after PWMI. We did not find significant difference in cCas3 expression in MAG^+ OLs after PWMI at P14, suggesting that the apoptosis of OLs is not altered at this time point. Although cCasp3 expression is not an indicator for apoptosis

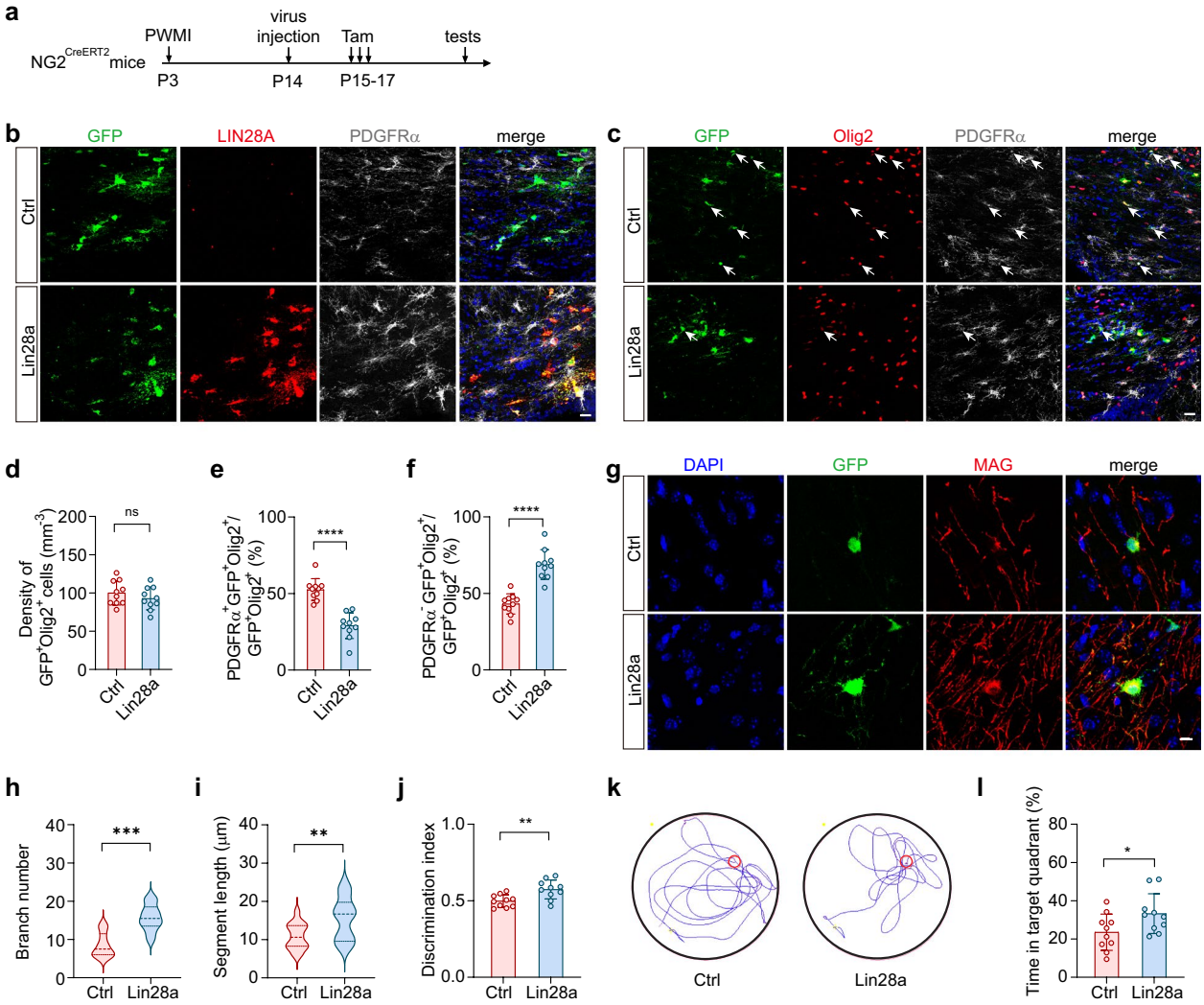

Fig. 5 Overexpressing *Lin28a* in OPCs rescued myelinogenesis and cognitive functions in PWMI mice. **a** Experimental schematics. **b** Representative images showing specific overexpression of LIN28A in OPCs. Scale bar: 20 μm. **c** Representative images showing the Olig2$^+$PDGFRα$^+$ cells in GFP$^+$ cells. Arrows indicate Olig2$^+$PDGFRα$^+$GFP$^+$ cells. Scale bar: 20 μm. **d** No significant difference was found in the density of Olig2$^+$GFP$^+$ cells between both groups (Ctrl n = 10 mice, Lin28a n = 10 mice; unpaired *t* test, $P = 0.3073$). **e** Overexpression of *Lin28a* decreased the proportion of Olig2$^+$PDGFRα$^+$GFP$^+$ cells among Olig2$^+$GFP$^+$ cells (Crtl n = 10 mice, Lin28a n = 10 mice; unpaired *t* test, $^{****}P < 0.0001$). **f** Overexpression of *Lin28a* increased the proportion of Olig2$^+$PDGFRα$^-$GFP$^+$ cells among Olig2$^+$GFP$^+$ cells (Crtl n = 10 mice, Lin28a n = 10 mice; unpaired *t* test, $^{****}P < 0.0001$). **g** Representative images showing virally labeled OLs. Scale bar: 10 μm. **h** Overexpressing *Lin28a* led to increased number of branches from single OLs in PWMI mice. (Ctrl n = 50 cells from 5 mice, Lin28a n = 50 cells from 5 mice; unpaired *t* test, $^{***}P = 0.0001$). **i** Overexpressing *Lin28a* led to increased segment length of myelin sheaths in PWMI mice (Ctrl n = 75 cells from 5 mice, Lin28a n = 75 cells from 5 mice; unpaired t test, $^{**}P = 0.0090$). **j** Overexpressing *Lin28a* rescued NOR in PWMI mice (Ctrl n = 10 mice, Lin28a n = 10 mice; unpaired t test, $^{**}P = 0.0048$). **k** Representative swimming traces of mice in the Morris water maze during the test session. The red circle indicates the location of the platform during training sessions. **l** Overexpressing *Lin28a* increased the time that PWMI mice spent in the target quadrant during the water maze test session. (Ctrl n = 10 mice, Lin28a n = 10 mice; unpaired *t* test, $^{*}P = 0.0429$). Data are shown as Mean ± SD

under certain conditions, such as hypoxia/ischemia [27], we examined cCasp3 more than 10 days post PWMI procedure, excluding the possibility of cCasp3 expression in non-apoptotic cells right after hypoxia/ischemia. Given that PWMI does not lead to excessive death of OLs, the decreased mature myelinating OLs and increased undifferentiated OPCs after PWMI indicate arrested differentiation of OPCs and hindered maturation of OLs. These defects have been considered as the main cause of the impaired grey matter connectivity by hypomyelination in PWMI [28, 29]. Although the exact mechanisms remain unclear, potential factors may include accumulation of hyaluronic acid triggered by excessive secretion from reactive astrocytes, chronic

activation of microglia, and alterations in the cell cycle of OPCs, etc. [30]. Acting in concert, these factors disrupt the normal differentiation of OPCs and maturation of OLs, thereby leading to impaired myelination.

In the mammalian central nervous system, the RNA-binding protein LIN28 is expressed during early developmental stages, but rapidly decreases by E10.5 [9]. Differential expression of the two homologs of LIN28, LIN28A and LIN28B, has also been reported in the mammalian brain [31]. It has been reported that LIN28B/*let-7* in Schwann cells regulates the myelination of peripheral nerves. Developmental repression of LIN28B leads to accumulation of *let-7* and consequently drives the onset of myelination by suppressing Notch signaling [13]. Using RNAscope to analyze the relative expression levels in single cells, we identified LIN28A as the dominating LIN28 homolog in OPCs in the postnatal brain, and its expression gradually decreases with development. Interestingly, we found that the expression of *Lin28a* exhibited an accelerated decrease in OPCs following PWMI, suggesting that the reduced expression of *Lin28a* may be involved in the defects in differentiation of OPCs and maturation of OLs in PWMI. By knockout of *Lin28a* gene in OPCs, we found that OPC differentiation and OL maturation were both impeded, similar to the impaired myelinogenesis in PWMI. These data suggest that LIN28A may play an important role for regulating these processes in myelinogenesis, in a dose-dependent manner. However, we did not observe changes in the number of tdTomato-labeled OPCs/OLs, indicating that the proliferation of OPCs was not altered by the loss of LIN28A.

Accumulating evidence has demonstrated that myelination is required for motor and cognitive functions [32–34]. Defects in myelinogenesis after PWMI result in broad impairments in brain functions, including motor and cognitive disability [3, 4]. Compared to the NLR, which relies heavily on hippocampal activity, the NOR relies on multiple brain regions [35]. Given that myelination is critical for high-speed impulse propagation and information processing in the brain [36, 37], the hypomyelination in PWMI leads to deficits in NOR, rather than NLR, by impairing information communication between brain regions. Similarly, this myelination deficit also leads to impaired spatial memory and motor functions in the Morris water maze test.

In our study, we found that overexpression of LIN28A specifically in OPCs recovered myelinogenesis by facilitating differentiation of OPCs and maturation of OLs in PWMI mice. Functionally, these mice exhibited recovered cognitive functions in both NOR and Morris water maze test, suggesting that supplementing LIN28A in OPCs could at least partially rescue myelinogenesis in the PWMI mouse model.

Since overexpression of LIN28B in Schwann cells inhibits its myelination [13], while overexpression of LIN28A promotes OPC differentiation and OL maturation, the two LIN28 homologs may show different expression pattern and play distinct roles in the nervous system under different contexts. Through *let-7*-dependent and -independent mechanisms, LIN28 enhances translation of multiple genes and regulates cellular metabolism [7]. LIN28A may exert its pro-myelinogenesis effect by improving cellular bioenergetics and facilitating cellular maturation [7, 38, 39]. Although the underlying mechanisms require further investigation, our results indicate that overexpression of LIN28A in OPCs might be a potential strategy to promote myelinogenesis and cognitive recovery for the treatment of PWMI. In addition, given the difference in brain size and white matter content between rodents and gyrencephalic species including humans [40], further studies will be required to confirm whether the same mechanism is involved in large animals, and whether supplementing LIN28A is able to rescue brain function deficits in large animal models for PWMI.

Conclusions

Our study revealed that RNA-binding protein LIN28A is important in regulating myelinogenesis processes in the brain dose-dependently. Reduced expression of LIN28A in OPCs is associated with impeded myelinogenesis and impaired cognitive functions in PWMI. Supplementing LIN28A in OPCs could rescue myelinogenesis in the PWMI mouse model, providing a promising strategy to promote myelinogenesis and cognitive recovery for the treatment of PWMI.

Abbreviations

cCasp3	Cleaved caspase 3
EPM	Elevated plus-maze
MAG	Myelin-associated glycoprotein
NLR	Novel location recognition
NOR	Novel object recognition
OL	Oligodendrocyte
Olig2	Oligodendrocyte transcription factor 2
OPC	Oligodendrocyte precursor cell
PBS	Phosphate buffer solution
PDGFRα	Platelet-derived growth factor receptor α
PFA	Paraformaldehyde
PWMI	Preterm white matter injury
Tam	Tamoxifen

Supplementary Information

The online version contains supplementary material available at https://doi.org/10.1186/s13287-025-04267-9.

Additional file 1.

Acknowledgements
We are grateful to the Core Facilities of Zhejiang University School of Medicine for technical assistance. The authors declare that they have not used Artificial Intelligence in this study.

Author contributions
X.W. performed most of the experiments and analysis; Z.H. helped with experimental design and behavior tests; H.Y. conducted plasmid construction and helped with viral packaging; C.W. helped with behavior tests; J.L. performed some confocal imaging; Y.Y. and Z.L. helped with the experimental design; L.W. and Y.S. edited the manuscript and provided constructive comments; Y.G. supervised this study and wrote the manuscript.

Funding
National Key Research and Development Program of China, 2017YFA0104200, Yan Gu, National Natural Science Foundation of China, 32071021, Yan Gu, China National Funds for Distinguished Young Scientists, 32225021, Yan Gu.

Availability of data and materials
All data generated or analyzed during this study are included in this article and its supplementary information files.

Declarations

Ethics approval and consent to participate
A protocol was prepared before this study, and approved by the Animal Care and Use Committee at Zhejiang University School of Medicine. (1) Title of the approved project: The regulatory roles for LIN28A in neurogenesis and gliogenesis. (2) Name of the institutional approval committee: Animal Care and Use Committee at Zhejiang University School of Medicine. (3) Approval number: ZJU20200115. (4) Date of approval: Oct. 18, 2020.

Consent for publication
Not applicable.

Competing interest
The authors declare that they have no competing interests.

Received: 25 June 2024 Accepted: 4 March 2025
Published online: 18 March 2025

References

1. Volpe JJ. Cerebral white matter injury of the premature infant-more common than you think. Pediatrics. 2003;112(1 Pt 1):176–80.
2. Jarjour IT. Neurodevelopmental outcome after extreme prematurity: a review of the literature. Pediatr Neurol. 2015;52(2):143–52.
3. Khwaja O, Volpe JJ. Pathogenesis of cerebral white matter injury of prematurity. Arch Dis Child Fetal Neonatal Ed. 2008;93(2):F153–61.
4. Back SA, Riddle A, McClure MM. Maturation-dependent vulnerability of perinatal white matter in premature birth. Stroke. 2007;38(2 Suppl):724–30.
5. Back SA, Volpe JJ. Cellular and molecular pathogenesis of periventricular white matter injury. Ment Retard Dev D R. 1997;3(1):96–107.
6. Wang X, Zang J, Yang Y, Lu S, Guan Q, Ye D, et al. Transplanted human oligodendrocyte progenitor cells restore neurobehavioral deficits in a rat model of preterm white matter injury. Front Neurol. 2021;12: 749244.
7. Shyh-Chang N, Daley GQ. Lin28: primal regulator of growth and metabolism in stem cells. Cell Stem Cell. 2013;12(4):395–406.
8. Thornton JE, Gregory RI. How does Lin28 let-7 control development and disease? Trends Cell Biol. 2012;22(9):474–82.
9. Balzer E, Heine C, Jiang Q, Lee VM, Moss EG. LIN28 alters cell fate succession and acts independently of the let-7 microRNA during neurogliogenesis in vitro. Development. 2010;137(6):891–900.
10. Hu Z, Ma J, Yue H, Luo Y, Li X, Wang C, et al. Involvement of LIN28A in Wnt-dependent regulation of hippocampal neurogenesis in the aging brain. Stem Cell Rep. 2022;17(7):1666–82.
11. Xia XH, Ahmad I. let-7 microRNA regulates neurogliogenesis in the mammalian retina through Hmga2. Dev Biol. 2016;410(1):70–85.
12. Patterson M, Gaeta X, Loo K, Edwards M, Smale S, Cinkornpumin J, et al. let-7 miRNAs can act through notch to regulate human gliogenesis. Stem Cell Rep. 2014;3(5):758–73.
13. Gokbuget D, Pereira JA, Bachofner S, Marchais A, Ciaudo C, Stoffel M, et al. The Lin28/let-7 axis is critical for myelination in the peripheral nervous system. Nat Commun. 2015;6.
14. Chen Q, Zhang K, Wang M, Gao R, Wang Q, Xiao M, et al. A translational mouse model for investigation of the mechanism of preterm diffuse white matter injury. Transl Pediatrics. 2022;11(7):1074–84.
15. Ma J, Hu Z, Yue H, Luo Y, Wang C, Wu X, et al. GRM2 regulates functional integration of adult-born DGCs by paradoxically modulating MEK/ERK1/2 pathway. J Neurosci: Off J Soc Neurosci. 2023;43(16):2822–36.
16. Gu Y, Arruda-Carvalho M, Wang J, Janoschka SR, Josselyn SA, Frankland PW, et al. Optical controlling reveals time-dependent roles for adult-born dentate granule cells. Nat Neurosci. 2012;15(12):1700–6.
17. Vannucci SJ, Hagberg H. Hypoxia-ischemia in the immature brain. J Exp Biol. 2004;207(Pt 18):3149–54.
18. Du MJ, Wang N, Xin XL, Yan CL, Gu Y, Wang L, et al. Endothelin-1-Endothelin receptor B complex contributes to oligodendrocyte differentiation and myelin deficits during preterm white matter injury. Front Cell Dev Biol. 2023;11.
19. Tsialikas J, Romer-Seibert J. LIN28: roles and regulation in development and beyond. Development. 2015;142(14):2397–404.
20. Ophelders D, Gussenhoven R, Klein L, Jellema RK, Westerlaken RJJ, Hutten MC, et al. Preterm brain injury, antenatal triggers, and therapeutics: timing is key. Cells. 2020;9(8):1871.
21. van Tilborg E, Achterberg EJM, van Kammen CM, van der Toorn A, Groenendaal F, Dijkhuizen RM, et al. Combined fetal inflammation and postnatal hypoxia causes myelin deficits and autism-like behavior in a rat model of diffuse white matter injury. Glia. 2018;66(1):78–93.
22. Motavaf M, Piao X. Oligodendrocyte development and implication in perinatal white matter injury. Front Cell Neurosci. 2021;15: 764486.
23. Liu XB, Shen Y, Plane JM, Deng W. Vulnerability of premyelinating oligodendrocytes to white-matter damage in neonatal brain injury. Neurosci Bull. 2013;29(2):229–38.
24. Zeng Y, Wang H, Zhang L, Tang J, Shi J, Xiao D, et al. The optimal choices of animal models of white matter injury. Rev Neurosci. 2019;30(3):245–59.
25. Ge Y, Zhen F, Liu Z, Feng Z, Wang G, Zhang C, et al. Alpha-asaronol alleviates dysmyelination by enhancing glutamate transport through the activation of PPARgamma-GLT-1 signaling in hypoxia-ischemia neonatal rats. Front Pharmacol. 2022;13: 766744.
26. Wang J, He X, Meng H, Li Y, Dmitriev P, Tian F, et al. Robust myelination of regenerated axons induced by combined manipulations of GPR17 and microglia. Neuron. 2020;108(5):876-86.e4.
27. Wagner DC, Riegelsberger UM, Michalk S, Hartig W, Kranz A, Boltze J. Cleaved caspase-3 expression after experimental stroke exhibits different phenotypes and is predominantly non-apoptotic. Brain Res. 2011;1381:237–42.
28. Buser JR, Maire J, Riddle A, Gong X, Nguyen T, Nelson K, et al. Arrested preoligodendrocyte maturation contributes to myelination failure in premature infants. Ann Neurol. 2012;71(1):93–109.
29. Riddle A, Dean J, Buser JR, Gong X, Maire J, Chen K, et al. Histopathological correlates of magnetic resonance imaging-defined chronic perinatal white matter injury. Ann Neurol. 2011;70(3):493–507.
30. Back SA, Rosenberg PA. Pathophysiology of glia in perinatal white matter injury. Glia. 2014;62(11):1790–815.
31. Yang M, Yang SL, Herrlinger S, Liang C, Dzieciatkowska M, Hansen KC, et al. Lin28 promotes the proliferative capacity of neural progenitor cells in brain development. Development. 2015;142(9):1616–27.
32. McKenzie IA, Ohayon D, Li H, de Faria JP, Emery B, Tohyama K, et al. Motor skill learning requires active central myelination. Science. 2014;346(6207):318–22.
33. Steadman PE, Xia F, Ahmed M, Mocle AJ, Penning ARA, Geraghty AC, et al. Disruption of oligodendrogenesis impairs memory consolidation in adult mice. Neuron. 2020;105(1):150–646.
34. Pan S, Mayoral SR, Choi HS, Chan JR, Kheirbek MA. Preservation of a remote fear memory requires new myelin formation. Nat Neurosci. 2020;23(4):487–99.

35. Denninger JK, Smith BM, Kirby ED. Novel Object Recognition and Object Location Behavioral Testing in Mice on a Budget. J Vis Exp: JoVE. 2018(141).
36. Moore S, Meschkat M, Ruhwedel T, Trevisiol A, Tzvetanova ID, Battefeld A, et al. A role of oligodendrocytes in information processing. Nat Commun. 2020;11(1):5497.
37. Bonetto G, Belin D, Karadottir RT. Myelin: a gatekeeper of activity-dependent circuit plasticity? Science. 2021;374(6569):eaba6905.
38. Shyh-Chang N, Zhu H, Yvanka de Soysa T, Shinoda G, Seligson MT, Tsanov KM, et al. Lin28 enhances tissue repair by reprogramming cellular metabolism. Cell. 2013;155(4):778–92.
39. Vogt EJ, Meglicki M, Hartung KI, Borsuk E, Behr R. Importance of the pluripotency factor LIN28 in the mammalian nucleolus during early embryonic development. Development. 2012;139(24):4514–23.
40. Boltze J, Nitzsche F, Jolkkonen J, Weise G, Posel C, Nitzsche B, et al. Concise review: increasing the validity of cerebrovascular disease models and experimental methods for translational stem cell research. Stem Cells. 2017;35(5):1141–53.

Publisher's Note